

would seem to indicate that the spin conservation rule is still applicable for this reaction. There is evidence, however, that there is breakdown in the LS coupling scheme for the $4F$ states. Abrams and Wolga⁸ have measured considerable transfer in the case of $4^3F \rightarrow 4^1D$ relative to $4^3F \rightarrow 4^3D$. This of course is a different reaction. A glance at estimates of the spin-orbit interaction compared with the electrostatic repulsion interaction⁹ shows that $4P$ is a good LS coupling

term, $4D$ is poorer while $4F$ is the poorest. Thus the reaction, $4^3F \rightarrow 4^1D$, involves the pair of collision partners least likely to obey the spin conservation rules. A further consideration is that 4^1P , 4^3F energy separation is over 6 times larger than the 4^1D , 4^3F separation and thus the 4^1D , 4^3F collision represents a nearer resonance reaction; however, both separations are smaller than thermal energies.

*Supported by the National Science Foundation.

†National Defense Education Act Title IV Predoctoral Fellow.

¹R. M. St. John, F. L. Miller, and C. C. Lin, *Phys. Rev.* **134**, A888 (1964).

²J. D. Jobe and R. M. St. John, *J. Opt. Soc. Am.* **57**, 1449 (1967).

³R. B. Kay and R. H. Hughes, *Phys. Rev.* **154**, 61 (1967).

⁴W. R. Pendleton, *Rev. Sci. Instr.* **36**, 1645 (1965).

⁵S. Chung and C. C. Lin, *Bull. Am. Phys. Soc.* **13**, 214 (1968).

⁶However, it is to be noted that the present experi-

mental measurements are relative and that the resulting absolute direct excitation cross sections are dependent upon the values of the absolute apparent cross sections to which the relative data are normalized. At present there exist several sources of absolute excitation cross-section data, e.g., see B. L. Moiseiwitsch and S. J. Smith, *Rev. Mod. Phys.* **40**, 238 (1968).

⁷R. M. St. John and T. Nee, *J. Opt. Soc. Am.* **55**, 426 (1965).

⁸R. L. Abrams and G. J. Wolga, *Phys. Rev. Letters* **19**, 1411 (1967).

⁹C. C. Lin and R. G. Fowler, *Ann. Phys. (N.Y.)* **15**, 461 (1961).

Generalized Oscillator Strengths of the Helium Atom. II. Transitions from the Metastable States*

Yong-Ki Kim and Mitio Inokuti

Argonne National Laboratory, Argonne, Illinois 60439

(Received 13 January 1969)

The generalized oscillator strengths for the transitions $2^1S \rightarrow 2^1P$, 3^1S , 3^1P , 3^1D , 4^1P , and $2^3S \rightarrow 2^3P$, 3^3S , 3^3P , 3^3D , 4^3P of He are computed from the Weiss correlated wave functions of the Hylleraas type. The results from two alternative formulas, corresponding to the "length" and "velocity" formulas in the optical limit, agree with each other within a few percent for moderate values of the momentum transfer. The first Born excitation cross sections for the above-mentioned transitions by charged-particle impact are also presented.

1. INTRODUCTION

Although the metastable 2^1S and 2^3S states of the helium atom play important roles in various gaseous phenomena as unique species by virtue of their long radiative lifetimes^{1,2} and great reactivity,³ current information on the inelastic scattering of charged particles by the metastable He atoms is quite limited.⁴⁻⁷ We have, there-

fore, extended our earlier work on some transitions from the ground state⁸ to include the generalized oscillator strengths for the $2^1S \rightarrow 2^1P$, 3^1S , 3^1P , 3^1D , 4^1P and $2^3S \rightarrow 2^3P$, 3^3S , 3^3P , 3^3D , 4^3P excitations. The Born cross sections^{8,9} for the excitations by charged-particle impact are also presented.

We have used correlated wave functions by Weiss¹⁰ as before, and we believe our results to

be accurate to 5% or better; thus they should serve as means to test the validity of the Born approximation whenever experimental data in the pertinent velocity region become available. Moreover we may propose the use of our results for analytical purposes. For example, a beam containing metastable He atoms as produced in the laboratory by electron impact¹¹ usually consists of three species, 2¹S, 2³S, and 1¹S; the concentration of the respective species can now be determined by combining our calculated generalized oscillator strengths with energy-loss spectra measured with sufficiently fast electrons.

We hope that our results will be useful also in astrophysics, for example, in the analysis of the population of the metastable He atoms in gaseous nebulae.^{12,13}

2. DEFINITIONS

The generalized oscillator strength $f_n(K)$ for the transition of an N -electron atom from state 0 to state n at momentum transfer $\vec{K}\hbar$ is given by^{8,9}

$$f_n(K) = [(E_n/R)/(Ka_0)^2] \times \left| \sum_{j=1}^N \int \psi_n^* e^{i\vec{K}\cdot\vec{r}_j} \psi_0 d\vec{r}_1 \cdots d\vec{r}_N \right|^2, \quad (1)$$

where a_0 is the Bohr radius, R the Rydberg energy, E_n the excitation energy, \vec{r}_j the position of the j th electron, and ψ_n and ψ_0 are the wave functions of the final and initial states, respectively. When the states involved are degenerate, customary average and summation over substates are implied. The notations here and below are the same as in our Paper I of this series, except that we must specify here the initial state 2¹S or 2³S. The transitions dealt with are all between states with the same spin multiplicity, for the generalized oscillator strength otherwise vanishes unless one allows for spin-dependent couplings, which are all weak in He. Where necessary, we shall denote the singlet transitions by a superscript + on the left, and the triplet transitions by -. For instance, $^+f_{3^1S}(K)$ is the generalized oscillator strength for the 2¹S → 3¹S transition, and $^-f_{3^3P}(K)$ that for the 2³S → 3³P transition.

An alternative formula to Eq. (1) is¹⁴

$$f_n(K) = (R/E_n) a_0^2 \times \left| \sum_{j=1}^N \int e^{iKz_j} \left(\psi_n^* \frac{\partial \psi_0}{\partial z_j} - \psi_0 \frac{\partial \psi_n^*}{\partial z_j} \right) d\vec{r}_1 \cdots d\vec{r}_N \right|^2, \quad (2)$$

where $z_j = (\vec{K} \cdot \vec{r}_j)/K$. In the limit $K \rightarrow 0$, Eqs. (1) and (2) reduce to the "length" and "velocity"

formulas for the optical (dipole) oscillator strength f_n , respectively.

The differential cross section for inelastic scattering of a particle of charge ze and velocity v with concomitant excitation (or de-excitation) of an atom from state 0 to n is given, in the first Born approximation, by^{9,15}

$$d\sigma_n = \frac{4\pi a_0^2 z^2}{T/R} \frac{f_n(K)}{E_n/R} d\ln(Ka_0)^2, \quad (3)$$

where $T = m_e v^2/2$ and m_e is the electron mass.

The generalized oscillator strength may be expressed in terms of a power series in $(Ka_0)^2$ provided $(Ka_0)^2$ is sufficiently small:

$$f_n(K) = \sum_{\lambda=0}^{\infty} (Ka_0)^{2\lambda} f_n^{(\lambda)}/\lambda!, \quad (4)$$

where the coefficients $f_n^{(\lambda)}$ depend on the matrix elements of $\sum_j z_j^\mu$ and μ takes on the values 1, 2, ..., $2\lambda + 1$. [See Eq. (5) of Paper I.]

The wave functions that we have used are due to Weiss,¹⁰ and have the form (specified by the usual quantum numbers n , l , and m)

$${}^\pm \psi_{nlm} = \sum_{pq\mu} {}^\pm c_{pq\mu, n} {}^\pm \phi_{pq\mu, lm} \quad (5)$$

with

$${}^\pm \phi_{pq\mu, lm} = 2^{-\frac{1}{2}} \zeta^{p+q+\mu+3+l} \left| \vec{r}_1 - \vec{r}_2 \right|^\mu \times [r_1^p r_2^{q+l} e^{-\zeta(r_1+\eta r_2)} Y_{00}^{(1)} Y_{lm}^{(2)} \mp r_1^{q+l} r_2^p e^{-\zeta(r_2+\eta r_1)} Y_{lm}^{(1)} Y_{00}^{(2)}], \quad (6)$$

where + and - stand for the singlet and triplet states, respectively, the quantities p , q , and μ are nonnegative integers, and ${}^\pm c_{pq\mu, n}$, ζ , and η are variational parameters. As to the procedures of computing $f_n(K)$ by Eq. (1) or (2), refer to Sec. 3 of Paper I.

It is now well recognized that one usually needs accurate wave functions for reliable evaluation of the generalized oscillator strengths. The Weiss wave functions compare very favorably with more elaborate ones calculated by Pekeris and co-workers,¹⁶ as can readily be judged from the energies and other properties¹⁷ listed in Table I.

The excitation cross section σ_n is obtained by integrating Eq. (3) between kinematical limits of K . For sufficiently large T , for which the Born approximation is valid, σ_n can be conveniently parameterized by the Bethe procedure.^{8,9,15} The result is

TABLE I. Comparison of properties calculated from the Weiss wave functions¹⁰ with those from the Pekeris wave functions.¹⁶ (a. u.)

Properties	Source	Singlet states				Triplet states					
		Initial 2 ¹ S	2 ¹ P	3 ¹ S	Final state 3 ¹ P	Initial 2 ³ S	2 ³ P	Final state 3 ³ S	3 ³ P	3 ³ D	4 ³ P
Number of terms in wave function	Weiss	54	52	54	52	18	52	54	52	52	18
	Pekeris	615	560	220	560	560	560	220	560	560	560
Excitation energy, non-relativistic ^a	Weiss	2.145 971	0.022 131	0.084 716	0.090 840	0.090 354	0.115 019	2.175 229	0.042 066	0.106 542	0.117 168
	Pekeris	2.145 974	0.022 131	0.084 703	0.090 828	0.114 904	0.114 904	2.175 229	0.042 065	0.106 540	0.117 148
Expectation value of r_1^2	Weiss	16.084	15.755	85.770	91.966	63.178	294.86	11.465	13.208	68.714	82.166
	Pekeris	16.089	15.766		91.873		304.06	11.464	13.212	82.110	82.110
Expectation value of r_2^2	Weiss	32.293	31.578	171.60	183.98	126.42	589.72	23.047	26.636	137.49	164.42
	Pekeris	32.302	31.599		183.79		608.14	23.046	26.643	164.30	164.30
Optical oscillator strength (length form)	Weiss		0.3764		0.1478		0.0508		0.5391		0.0641
	Schiff ^b		0.3764		0.1514				0.5391		0.0645
Optical oscillator strength (velocity form)	Weiss		0.3774		0.1506		0.0506		0.5401		0.0634
	Schiff ^b		0.3764		0.1514				0.5391		0.0645
Overlap with the initial state	Weiss			-1.1×10^{-3}							2.0×10^{-5}

^aTotal energies are given for the initial states.^bThe oscillator strengths by Schiff and Pekeris (Ref. 18) are calculated from 220-term wave functions.

$$\sigma_s = \frac{4\pi a_0^2 z^2}{T/R} \left[\frac{f_s}{E_s/R} \ln \frac{4c_s T}{R} + \frac{\gamma_s}{T/R} + O\left(\frac{E_s^2}{T^2}\right) \right] \quad (7)$$

for an allowed transition ($n=s$), and

$$\sigma_{s'} = \frac{4\pi a_0^2 z^2}{T/R} \left[b_{s'} + \frac{\gamma_{s'}}{T/R} + O\left(\frac{E_{s'}^2}{T^2}\right) \right] \quad (8)$$

for a forbidden transition ($n=s'$). The parameters c_s , γ_s , $b_{s'}$, and $\gamma_{s'}$ are all evaluated from the generalized oscillator strength by means of Eqs. (12), (13), (15), and (16) of Paper I.

3. RESULT AND DISCUSSION

The generalized oscillator strengths for the singlet and triplet transitions are presented in Tables II and III, respectively. The values in the "Formula I" columns were computed from Eq. (1), and those in the "Formula II" columns from Eq. (2). The excitation energies computed by Weiss were used in both cases. The agreement between "Formula I" and "Formula II" results is typically 3% or better in the region where the magnitudes of $\pm f_n(K)$ are significant. As we mentioned in Paper I, "Formula I" results are more reliable for large momentum transfers [$(Ka_0 \geq 0.5)$].

TABLE II. Generalized oscillator strengths $\pm f_n(K) \times 10^3$ for the singlet transitions from the 2^1S state of He [see Eqs. (1) and (2)].

n Formula (Ka_0) ²	2 ¹ P		3 ¹ S		3 ¹ P		3 ¹ D		4 ¹ P	
	I ^a	II	I	II	I	II	I	II	I	II
0.001	373.0	374.2	6.022 ^b	2.430	142.8	145.4	5.835	5.903	49.82	49.61
0.005	360.5	361.7	14.01	11.43	124.0	125.9	27.65	27.95	45.75	45.90
0.01	345.6	346.7	23.32	21.17	103.4	104.7	51.73	52.23	40.97	41.47
0.02	317.6	318.6	37.98	36.36	70.39	70.87	90.61	91.29	32.40	33.36
0.04	268.7	269.6	54.94	53.81	29.07	28.90	139.5	140.1	19.02	20.25
0.06	227.8	228.6	60.94	59.98	9.094	8.872	162.0	162.3	10.00	11.09
0.08	193.5	194.2	60.54	59.65	1.304	1.206	168.0	168.0	4.437	5.227
0.10	164.6	165.3	56.65	55.80	0.1060	0.1354	164.1	163.9	1.417	1.895
0.15	110.8	111.3	41.77	41.11	7.258	7.411	135.5	135.3	0.2880	0.1175
0.20	75.27	75.74	27.77	27.33	14.74	14.87	102.1	102.1	2.571	1.966
0.25	51.57	51.97	17.47	17.21	18.29	18.38	73.92	74.01	4.814	3.942
0.30	35.60	35.93	10.60	10.46	18.56	18.66	52.51	52.66	6.063	5.054
0.35	24.72	25.00	6.257	6.171	16.97	17.10	37.00	37.15	6.361	5.317
0.40	17.25	17.49	3.596	3.540	14.59	14.73	26.00	26.12	6.022	5.011
0.45	12.09	12.29	2.008	1.967	12.05	12.19	18.28	18.37	5.345	4.408
0.50	8.496	8.657	1.083	1.050	9.685	9.819	12.88	12.94	4.544	3.701
0.55	5.980	6.113	0.5581	0.5309	7.635	7.756	9.104	9.141	3.747	3.005
0.60	4.211	4.319	0.2695	0.2479	5.931	6.037	6.457	6.479	3.021	2.377
0.65	2.962	3.049	0.1179	0.1019	4.555	4.645	4.596	4.610	2.394	1.842
0.70	2.079	2.149	0.0436	0.0330	3.464	3.540	3.282	3.292	1.872	1.403
0.75	1.453	1.508	0.0114	0.0059	2.613	2.676	2.352	2.360	1.446	1.051
0.80	1.009	1.053	0.000 91	3×10^{-6}	1.954	2.008	1.690	1.698	1.106	0.7749
0.85	0.6954	0.7286	0.000 69	0.0036	1.450	1.496	1.217	1.225	0.8381	0.5622
0.90	0.4736	0.4989	0.0045	0.0105	1.067	1.106	0.8779	0.8867	0.6290	0.4008
0.95	0.3178	0.3366	0.0091	0.0174	0.7777	0.8111	0.6343	0.6432	0.4675	0.2800
1.0	0.2090	0.2228	0.0131	0.0229	0.5607	0.5896	0.4586	0.4673	0.3439	0.1910
1.2	0.0263	0.0293	0.0170	0.0281	0.1292	0.1452	0.1244	0.1307	0.0873	0.0271
1.4	7×10^{-7}	0.000 04	0.0106	0.0187	0.0167	0.0235	0.0317	0.0351	0.0141	4×10^{-6}
1.6	0.0076	0.0068	0.0042	0.0087	0.000 03	0.000 42	0.0067	0.0081	0.000 16	0.0087
1.8	0.0177	0.0163	0.000 79	0.0026	0.0069	0.0032	0.000 81	0.0012	0.0025	0.0218
2.0	0.0242	0.0218	7×10^{-6}	0.000 22	0.0160	0.0098	2×10^{-6}	6×10^{-6}	0.0073	0.0315

^a"Formula I" results are calculated from Eq. (1), and "Formula II" results from Eq. (2).

^bExpansion formula (4) should be used for $(Ka_0)^2 \leq 0.12$.

TABLE III. Generalized oscillator strengths $^{-}f_n(K) \times 10^3$ for the triplet transitions from the 2^3S state of He [see Eqs. (1) and (2)].

n Formula (Ka_0) ²	2^3P		3^3S		3^3P		3^3D		4^3P	
	I ^a	II	I	II	I	II	I	II	I	II
0.001	535.6	536.6	1.685 ^b	1.639	61.85	61.16	3.514	3.462	23.52	21.73
0.005	521.6	522.6	7.861	7.821	53.53	52.88	16.78	16.53	21.56	19.87
0.01	504.7	505.7	14.80	14.76	44.36	43.76	31.69	31.20	19.26	17.68
0.02	472.7	473.7	26.33	26.30	29.61	29.11	56.59	55.65	15.13	13.75
0.04	415.2	416.2	41.89	41.86	11.13	10.82	90.51	88.84	8.654	7.632
0.06	365.3	366.2	50.15	50.12	2.600	2.452	109.1	106.8	4.302	3.590
0.08	322.0	322.7	53.53	53.51	0.0418	0.0251	117.3	114.7	1.673	1.237
0.10	284.1	284.9	53.72	53.69	0.8854	0.9723	118.8	115.9	0.3608	0.1741
0.15	209.3	209.9	47.04	47.02	8.556	8.809	107.2	103.9	0.5921	0.9212
0.20	155.4	156.0	37.12	37.11	16.23	16.57	87.85	84.57	2.879	3.587
0.25	116.3	116.8	27.78	27.78	20.93	21.31	68.91	65.78	5.213	6.185
0.30	88.70	88.12	20.15	20.15	22.75	23.14	52.87	49.97	6.864	8.005
0.35	66.55	66.92	14.32	14.31	22.52	22.91	40.11	37.48	7.724	8.961
0.40	50.80	51.12	10.02	10.01	21.05	21.43	30.27	27.91	7.930	9.207
0.45	38.99	39.27	6.931	6.921	18.97	19.33	22.81	20.71	7.676	8.951
0.50	30.07	30.32	4.741	4.729	16.66	17.00	17.20	15.35	7.139	8.380
0.55	23.30	23.51	3.207	3.196	14.37	14.69	13.00	11.36	6.454	7.641
0.60	18.12	18.31	2.145	2.135	12.24	12.54	9.849	8.416	5.716	6.834
0.65	14.15	14.31	1.415	1.406	10.33	10.62	7.487	6.235	4.984	6.026
0.70	11.08	11.22	0.9187	0.9113	8.654	8.927	5.712	4.619	4.296	5.257
0.75	8.705	8.818	0.5846	0.5788	7.213	7.473	4.375	3.422	3.669	4.550
0.80	6.854	6.950	0.3627	0.3583	5.989	6.236	3.362	2.533	3.112	3.914
0.85	5.408	5.488	0.2175	0.2144	4.957	5.191	2.594	1.873	2.624	3.352
0.90	4.274	4.341	0.1246	0.1225	4.093	4.316	2.009	1.382	2.203	2.860
0.95	3.382	3.439	0.0668	0.0656	3.373	3.584	1.561	1.016	1.842	2.434
1.0	2.679	2.726	0.0324	0.0317	2.775	2.975	1.217	0.7444	1.536	2.067
1.2	1.055	1.078	0.00038	0.00036	1.255	1.411	0.4632	0.1984	0.7243	1.063
1.4	0.4060	0.4180	0.0113	0.0107	0.5545	0.6710	0.1834	0.0399	0.3302	0.5420
1.6	0.1458	0.1527	0.0186	0.0172	0.2360	0.3191	0.0745	0.0027	0.1446	0.2755
1.8	0.0447	0.0489	0.0191	0.0174	0.0939	0.1504	0.0306	0.0014	0.0594	0.1395
2.0	0.0093	0.0116	0.0161	0.0143	0.0328	0.0691	0.0125	0.0086	0.0218	0.0700

^a“Formula I” results are calculated from Eq. (1), and “Formula II” results from Eq. (2).

^bExpansion formula (4) should be used for small (Ka_0)².

For those $S \rightarrow P$ transitions for which accurate optical limits are known¹⁸ (Table I), we believe that the calculated results which lead to better agreement with such optical oscillator strengths are preferable. The results for the transitions to the 4^1P and 4^3P states are less trustworthy than the others because neither of the wave functions is as good as those used for other states (Table I).

For the $S \rightarrow S$ transitions, the “velocity” data (Formula II) are more reliable, partly because they are not affected by the nonorthogonality of the lower- and upper-state wave functions. The “length” results (Formula I) for the $2^1S \rightarrow 3^1S$ transition are strongly affected by the appreciable

overlap integral between the two wave functions (see Table I). For the $S \rightarrow D$ transitions the “length” results are probably better for (Ka_0)² ≥ 0.1 , particularly for the triplet transition.

In comparison with the $f_n(K)$ for the transitions from the ground state (see Paper I) we note: (a) that the magnitudes of $\pm f_n(K)$ for the (optically) allowed transitions are roughly twice those of the corresponding transitions from the ground state, and for the forbidden transitions almost one order of magnitude larger; (b) that the peaks of $\pm f_n(K)$ for the forbidden transitions are shifted toward smaller momentum transfers, that is, to the vicinity of (Ka_0)² ~ 0.1 ; and (c) that there are “zeros” of $\pm f_n(K)$ in all transitions, particularly

noticeable in the transitions to the $3P$ and $4P$ states, both singlet and triplet. Whenever the integral in Eq. (1) [or Eq. (2)] changes sign, a zero-value minimum of $\pm f_n(K)$ occurs. These minima are easily understood in terms of independent-particle models; their positions are closely related to the nodes of the radial functions of the states involved.¹⁹ For more complex atoms and molecules the minima of $f_n(K)$ are often observed in transitions from ground states.¹⁹

Although the occurrence of the minima is thus qualitatively interpreted, their quantitative aspects, for instance, the exact location of the minima, depend upon intricacies of the electronic structure such as electron correlation. In fact, the agreement between the "length" and "velocity" results, even from such elaborate wave functions as we have used, deteriorates near and beyond the first minimum because the minimum results from cancellation in the integrands of Eqs. (1) and (2). (See Tables II and III.)

As a consequence of the large magnitudes of $\pm f_n(K)$ for the low-lying excited states [see (a) above] and of the Bethe sum rule⁹ [$\sum n f_n(K) = N$ for any K], the shapes of the Bethe surfaces²⁰ for the metastables are very different from that for the normal He atom. The fact that the magnitudes of the $\pm f_n(K)$ for the forbidden transitions in the vicinity of $(Ka_0)^2 = 0.1$ become very large, while the minima of $\pm f_{3P}(K)$ and $\pm f_{4P}(K)$ occur in the same region, is consistent with the Bethe sum rule.

Note that the contribution of the region beyond the first minimum of $\pm f_{3P}(K)$ to the excitation cross section σ_S [Eq. (7)] is appreciable, as may be seen by plotting $\pm f_{3P}(K)$ against $\ln(Ka_0)^2$. [The area under such a curve between kinematic limits of $(Ka_0)^2$ is proportional to σ_S . (Ref. 15)].

The expansion coefficients [Eq. (4)] are given in Table IV. However, the range of validity of the expansion formula (4) is more limited than for transitions from the ground state.²¹ For the allowed transitions, Eq. (4) may be used only for $(Ka_0)^2$ much smaller than that at which the first minimum of $\pm f_n(K)$ occurs, and for the forbidden transitions it may not be used beyond the first maximum of $\pm f_n(K)$.

Our results for the $2^1S \rightarrow 2^1P$ and $2^3S \rightarrow 2^3P$ transitions may be used to analyze the composition of metastable He atoms produced experimentally. For instance, comparison of cross-section ratios of fast electrons for the two transitions (the excitation energies of which differ by 0.54 eV) at a few angles will readily determine the ratio of the metastable atoms present in the collision volume. In Figs. 1 and 2, we present the electron-impact energy-loss spectra for the 2^1S and 2^3S states, respectively, based on our calculated data. The height corresponds to the differential cross section per unit solid angle. We have not evaluated

TABLE IV. Power series expansion coefficients $f_n^{(\lambda)}/\lambda!$ [see Eq. (4)] for the generalized oscillator strengths of He.

Initial state	2^1S		2^3S		3^1S		3^3S		4^1P		4^3P		3^1D		3^3D		4^3P		
Final state	2^1P	3^1P	2^3P	3^3P	3^1S	3^3S	4^1P	4^3P	3^1D	3^3D	4^1P	4^3P	3^1D	3^3D	4^1P	4^3P	3^1D	3^3D	4^3P
$\lambda=0$	0.37637	0.14780	0.53912	0.06408			0.05087	0.53912			0.05087	0.53912			0.05087	0.53912			0.02402
1	-3.2055	-5.1185	-3.5651	-2.2597	2.3930	1.6567	-1.0572	-3.5651	5.9142	3.5544	-1.0572	-3.5651	5.9142	3.5544	-1.0572	-3.5651	5.9142	3.5544	-0.50751
2	14.670	73.171	12.978	30.971	-35.959	-19.303	6.6869	12.978	-79.580	-40.975	6.6869	12.978	-79.580	-40.975	6.6869	12.978	-79.580	-40.975	3.1266
3	-48.116	-602.55	-34.557	-229.70	279.91	119.40	4.7415	-34.557	574.37	257.98	4.7415	-34.557	574.37	257.98	4.7415	-34.557	574.37	257.98	2.9434
4	126.74	3468.0	75.274	1178.1	-1506.8	-523.75	-284.10	75.274	-2939.8	-1174.2	-284.10	75.274	-2939.8	-1174.2	-284.10	75.274	-2939.8	-1174.2	-128.79
5		6301.8		1631.4	6301.8	1631.4			11906.	4317.0			11906.	4317.0			4317.0	4317.0	

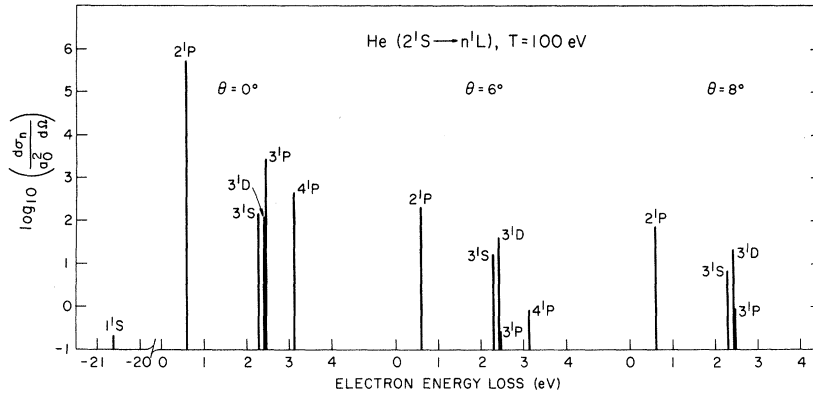


FIG. 1. Electron energy-loss spectra for the 2^1S He at an incident energy of 100 eV. The ordinate gives the differential cross section per unit solid angle in logarithmic scale. The 4^1P line for the scattering angle $\theta=8^\circ$ is too short to be seen. The 4^1S , 4^1D , and 4^1F lines are not included. The superelastic transition lines ($2^1S \rightarrow 1^1S$) at $\theta=6^\circ$ and 8° are similar in height to that for $\theta=0^\circ$.

the cross sections for the transitions to the $4S$, $4D$, and $4F$ states, either singlet or triplet, which should appear very close to those for the $4P$ states. Also, some singlet-triplet intercombination lines will appear in experimental spectra at low incident energies. The $2^1S \rightarrow 1^1S$ superelastic transition line is insignificant compared to other lines, at least in the high incident velocity range where the first Born approximation is valid. The zero-value minima of $\pm f_n(K)$ lead to the corresponding minima in the differential cross sections and hence may be used in identifying some transitions. These minima are responsible for the reduction or disappearance of the $3P$ lines at the scattering angle $\theta=6^\circ$ and the $4P$ lines at $\theta=8^\circ$ in Figs. 1 and 2. In reality, however, experimental cross sections may fail to vanish at the minima because of effects not included in the first Born approximation.¹⁹

At present, we are unaware of any experimental differential cross section to be compared with our results for metastable He atoms.

4. EXCITATION CROSS SECTIONS

The parameters for the excitation cross sections [Eqs. (7) and (8)] are listed in Table V. As is mentioned in Sec. 5 of Paper I, for an allowed transition γ_S depends on the reduced mass M of the incident particle and the atom, and in Table V

we list both $\gamma_S(e)$ for electrons and $\gamma_S^{(\infty)}$ for the case $M \rightarrow \infty$, a good approximation to protons and other heavy incident particles.

The asymptotic cross section [Eq. (7) or (8)] is not identical to "the Born cross section" which results from the integration of Eq. (3) between exact kinematical limits of K at a given T . However, the difference, which is represented by the remainder $O(E_n^2/T^2)$, is very small for the allowed transitions (less than 1% for electrons even at $T=5$ eV) and only a little larger for the forbidden transitions (1-2%). Some excitation cross sections for electrons computed from Eqs. (7), (8), and Table V are shown in Fig. 3 ($2^1S \rightarrow 2^1P$ and $2^3S \rightarrow 2^3P$), and Fig. 4 ($2^3S \rightarrow 3^3S$, 3^3P , and 3^3D). The ordinate of these figures represents $\sigma_n/(4\pi a_0^2)(T/R)$.

There are two earlier theoretical works on the excitation cross sections for the transitions from the 2^3S state. The calculation of Moiseiwitsch⁵ includes excitation cross sections for the $2^3S \rightarrow 2^3P$, 3^3P , and 3^3D transitions, and the calculation of Ochkur and Bratsev⁶ includes those for the $2^3S \rightarrow 3^3S$, 3^3P , and 3^3D transitions. Moiseiwitsch used modified hydrogenic wave functions to calculate Born cross sections. His 2^3P cross sections are in excellent agreement with ours (Fig. 3), but the 3^3P cross sections are larger than ours by about 10% and 3^3D cross section smaller by about 20% in the asymptotic region, as shown in

FIG. 2. Electron energy-loss spectra for the 2^3S He at an incident energy of 100 eV. The ordinate gives the differential cross section per unit solid angle in logarithmic scale. The 3^3P line at the scattering angle $\theta=6^\circ$ and 4^3P line at $\theta=8^\circ$ are too short to be seen. The 4^3S , 4^3D , and 4^3F lines are not included.

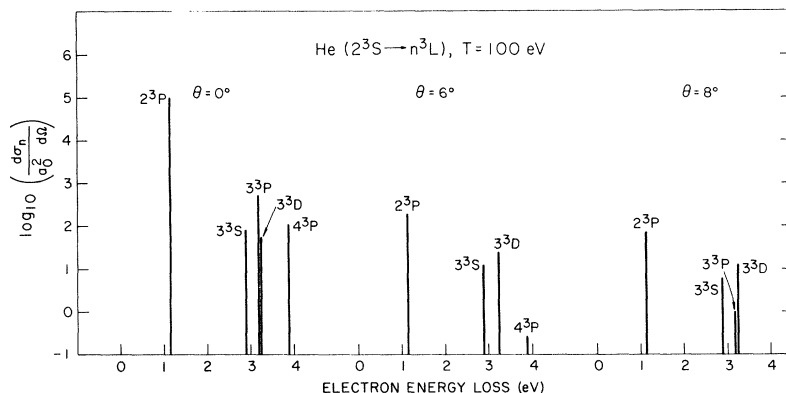


TABLE V. Parameters for the excitation cross sections [see Eqs. (7) and (8)].

Initial state	2^1S		2^3S			
Final state	2^1P	3^1P	A. Optically allowed transitions		3^3P	4^3P
			4^1P	2^3P		
$f_s/(E_s/R)$	8.503	0.814	0.221	6.408	0.273	0.084
$\text{In}c_s$	3.550	-0.662	-0.741	2.533	-0.878	-0.900
$\gamma_s^{(e)}$	-0.153	0.159	0.035	-0.195	0.100	0.024
$\gamma_s^{(\infty)}$	0.035	0.232	0.061	0.075	0.132	0.036
Final state	3^1S	3^1D	B. Optically forbidden transitions		3^3S	3^3D
b_s'	0.974	2.630			0.705	1.419
γ_s'	-0.101	-0.267			-0.088	-0.213

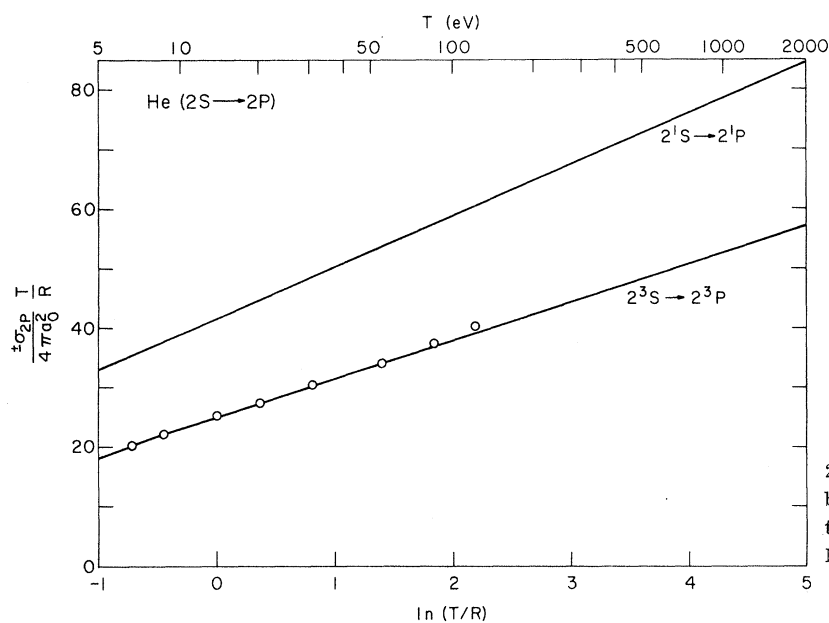


FIG. 3. Cross sections for the $2^1S \rightarrow 2^1P$ and $2^3S \rightarrow 2^3P$ transitions of He by electron impact. The circles (\circ) are the Born cross sections calculated by Moiseiwitsch (Ref. 5).

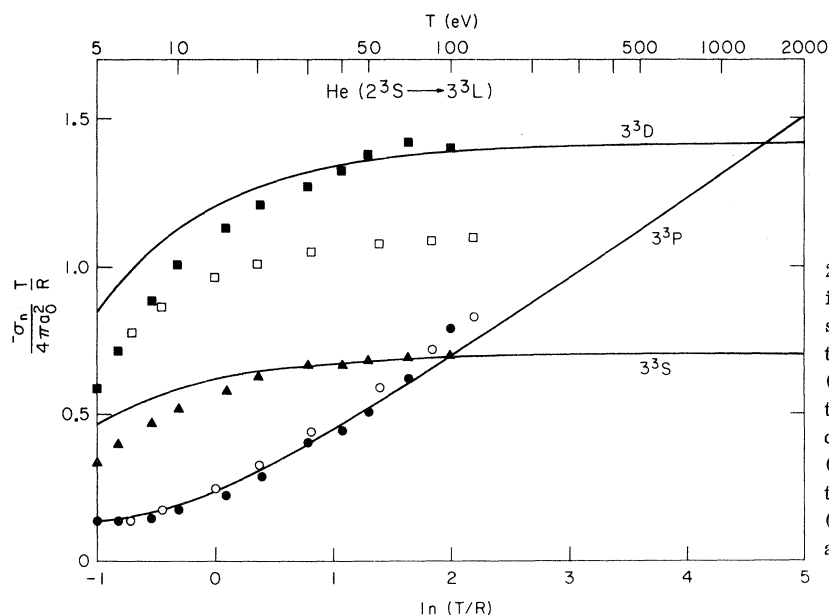


FIG. 4. Cross sections for the $2^3S \rightarrow 3^3L$ transitions of He by electron impact. The open circles (\circ) and squares (\square) are the Born cross sections calculated by Moiseiwitsch (Ref. 5) for the $2^3S \rightarrow 3^3P$ and $2^3S \rightarrow 3^3D$ transitions, respectively. The solid circles (\bullet), triangles (\blacktriangle) and squares (\blacksquare) are the Born-Ochkur cross sections calculated by Ochkur and Bratsev (Ref. 6), for the $2^3S \rightarrow 3^3P$, $2^3S \rightarrow 3^3S$ and $2^3S \rightarrow 3^3D$ transitions, respectively.

Fig. 4. On the other hand, Ochkur and Bratsev used Hartree-Fock wave functions and evaluated the cross sections with the Ochkur approximation to include the electron exchange effect. All of their cross sections are in essential agreement with our results except for the low incident energy region ($T \lesssim 20$ eV for electrons) where, for the forbidden transitions, the exchange effect appears to decrease the cross sections from the Born-approximation values (Fig. 4).

Since electron correlation is not expected to be strong in excited states of He, it is not surprising to find that the Hartree-Fock wave functions produce almost as accurate excitation cross sections as the correlated wave functions.

It is interesting to note in Fig. 4 that the Born excitation cross sections for the forbidden transitions ($2^3S \rightarrow 3^3S$ and 3^3D) are larger than that for the allowed transition ($2^3S \rightarrow 3^3P$) in the region $T < 100$ eV, contrary to the case of the transitions from the ground state^{8, 22} ($1^1S \rightarrow 3^1S$, 3^1P and 3^1D). For the singlet excitations from the 2^1S state only the 3^1D excitation exhibits a similar trend.

We expect the Born approximation for the tran-

sitions from the metastable states to be valid down to rather low incident velocities because the excitation energies are small, but there is at present no pertinent experimental information regarding the actual range of validity of the Born approximation. The result of a close-coupling calculation²³ appears to indicate that the asymptotic behavior of the cross sections, for the $2^1S \rightarrow 2^1P$ as well as $2^3S \rightarrow 2^3P$ transition, is attained at rather low incident electron energy, although the close-coupling results are somewhat smaller (by $\sim 20\%$ for the singlet and by $\sim 40\%$ for the triplet transitions) than the Born cross sections at $T = 15$ eV.

ACKNOWLEDGMENTS

The authors take this opportunity again to thank A. W. Weiss for providing the wave functions. They are indebted to J. W. Cooper and L. H. Aller for valuable communications, to F. F. Rieke for his critical review of the manuscript, and to D. Douthat for assistance in early stages of the work.

*Work performed under the auspices of the U. S. Atomic Energy Commission.

¹A. Dalgarno, *Monthly Notices Roy. Astron. Soc.* **131**, 311 (1966); G. W. F. Drake and A. Dalgarno, *Astrophys. J.* **152**, L121 (1968).

²O. Bely, *J. Phys. B.* **1**, 718 (1968).

³For instance, see Čermák and Z. Herman, *Collection Czech. Chem. Commun.* **30**, 169 (1965); V. Čermák, *J. Chem. Phys.* **44**, 3781 (1966), and references therein.

⁴Experimental data have so far been restricted to the threshold region. For example, see A. V. Phelps, *Phys. Rev.* **99**, 1307 (1955); F. Robben, W. B. Kunkel, and L. Talbot, *Phys. Rev.* **132**, 2363 (1963); and R. H. Neynaber *et al.*, *Atomic Collision Processes*, edited by M. R. C. McDowell (North-Holland Publishing Co., Amsterdam, 1964), p. 1089.

⁵B. L. Moiseiwitsch, *Monthly Notices Roy. Astron. Soc.* **117**, 189 (1957).

⁶V. I. Ochkur and V. F. Bratsev, *Astron. Zh.* **42**, 1034 (1965) [English transl.: *Soviet Astron. - AJ* **9**, 797 (1966)].

⁷R. Marriott, *Proc. Phys. Soc. (London)* **87**, 407 (1966).

⁸Y.-K. Kim and M. Inokuti, *Phys. Rev.* **175**, 176 (1968), referred to as Paper I hereafter.

⁹H. Bethe, *Ann. Physik* **5**, 325 (1930).

¹⁰A. W. Weiss, *J. Res. Natl. Bur. Std. (U.S.)* **71A**, 163 (1967).

¹¹For example, see V. Čermák, *J. Chem. Phys.* **44**, 3774 (1966); J. L. G. Dugan, H. L. Richard, and E. E. Muschlitz, Jr., *J. Chem. Phys.* **46**, 346 (1967); and

J. A. Herce, J. R. Penton, R. J. Cross, and E. E. Muschlitz, Jr., *ibid.* **49**, 958 (1968).

¹²D. E. Osterbrock, *Ann. Rev. Astronomy Astrophys.* **2**, 95 (1964).

¹³L. H. Aller and W. Liller, in *Stars and Stellar Systems*, edited by B. M. Middlehurst and L. H. Aller (The University of Chicago Press, Chicago, Illinois, 1968), Vol. VII, Chap. 9, Sec. 5.4.

¹⁴D. R. Bates, A. Fundaminsky, and H. S. W. Massey, *Phil. Trans. Roy. Soc. (London)* **A243**, 93 (1950).

¹⁵W. F. Miller and R. L. Platzman, *Proc. Phys. Soc. (London)* **A70**, 299 (1957).

¹⁶C. L. Pekeris, *Phys. Rev.* **115**, 1216 (1959); **126**, 1470 (1962); **127**, 509 (1962); and B. Schiff *et al.*, *ibid.* **140**, A1104 (1965).

¹⁷In the hydrogen atom, expectation values of r_l^{-2} for a given n are smaller the larger l is. In the helium atom, however, the $3S$ and $3P$ states, both singlet and triplet, deviate from the above pattern.

¹⁸B. Schiff and C. L. Pekeris, *Phys. Rev.* **134**, A638 (1964).

¹⁹Y.-K. Kim, M. Inokuti, G. E. Chamberlain, and S. R. Mielczarek, *Phys. Rev. Letters* **21**, 1146 (1968).

²⁰The Bethe surface is a comprehensive representation of the generalized oscillator strengths for all excitations from a given initial state; it is a three-dimensional plot of the differential generalized oscillator strength $[df(K, E)/dE$ for excitation energy $E]$ versus E and $\ln(Ka_0)^2$. For discrete transitions, it is convenient to replace $df(K, E)/dE$ by $f_n(K)(dn/dE_n)$ extended over the

interval $E_n - \Delta E_n \leq E \leq E_n + \Delta E_n$, where $\Delta E_n = \frac{1}{2}(dE_n/dn)$. Here, E_n is considered as a "smooth" function of quantum number n . See U. Fano and J. W. Cooper, *Rev. Mod. Phys.* **40**, 441 (1968), Sec. 2.4.

²¹For a qualitative understanding, Eq. (4) may be considered as an expansion of the exponential factor in Eq. (1) in an effective parameter Kr_{eff} , r_{eff} being a "transition radius" weighted by $\psi_n^* \psi_0$. For the transitions considered here, r_{eff} is much larger than it is

for the transitions from the ground state; therefore Eq. (4) is slower in convergence for a given K . For further discussion on the convergence, see E. N. Lassetre, *J. Chem. Phys.* **43**, 4479 (1965).

²²Y. -K. Kim and M. Inokuti, to be published. The $1^1S \rightarrow 3^1D$ excitation will be discussed in this reference.

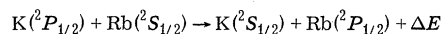
²³P. G. Burke, J. W. Cooper, and S. Ormonde, to be published.

Measured Absolute Cross Sections for $K^* + \text{Rb}$ Collisional Excitation Transfer*

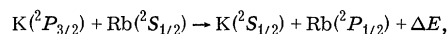
Michael H. Ornstein[†] and Richard N. Zare[‡]

*Department of Physics and Astrophysics, Joint Institute for Laboratory Astrophysics,
University of Colorado, Boulder, Colorado 80302*
(Received 27 January 1969)

The electronic excitation transfer processes,



and



have been studied by irradiating a cell containing a nonequilibrium mixture of potassium and rubidium vapors with either the 7665 Å D2 line or the 7699 Å D1 line of the potassium resonance doublet. The resulting collisionally induced rubidium 7948 Å fluorescence signal, isolated by interference filters used in tandem, is detected with a liquid-nitrogen-cooled S-1 photomultiplier placed at right angles to the direction of excitation. Measurements of the intensity ratio of the potassium and rubidium fluorescence combined with an optical absorption determination of the rubidium atom density yields the following excitation transfer cross sections:

$$Q[K(^2P_{1/2}) \rightarrow \text{Rb}(^2P_{1/2})] = 2.2 \text{ \AA}^2 \pm 25\%$$

and

$$Q[K(^2P_{3/2}) \rightarrow \text{Rb}(^2P_{1/2})] = 2.6 \text{ \AA}^2 \pm 20\%$$

at $T = 365^\circ \text{K} \pm 2\%$. Throughout an experimental run the potassium and rubidium vapor pressures are varied, but data are taken for only the lowest vapor pressures for which corrections due to resonance radiation imprisonment are unnecessary.

I. INTRODUCTION

When a gas gains energy by photo-excitation, electron impact, shock heating, radiolysis, chemical reaction, etc., appreciable concentrations of electronically excited atoms and molecules are often generated. These excited species may emit radiation, or they may be de-excited through various collisional encounters in which the energy is redistributed among the collision partners. The competition among the different deactivation pathways controls the subsequent physical behavior and chemical properties of the gas. Knowledge of the absolute cross sections (reaction rates) for energy transfer is thus of fundamental importance in understanding such diverse phenomena as flash

photolysis, flames, discharges, shocks, auroras, and stellar atmospheres. Among the various types of energy transfer, those between colliding atoms in different states of excitation are, in principle, some of the simplest. Of these, the excitation transfer between different alkali atoms has been of particular interest to us not only because such systems typify a large class of near-adiabatic inelastic processes, but also because these systems, which can be treated as hydrogen-like, offer promise of allowing a critical comparison between theory and experiment. We report here an experimental study of the interchange of electronic excitation between the lowest-lying excited states of potassium and rubidium in which cross sections for energy transfer between some of the fine-